4-1-2017

Characterization of pyridostatin and its interactions with c-MYC g-quadruplexes

Zachary G. Cuny

Characterization of Pyridostatin and its Interactions with c-MYC G-Quadruplexes

By

Zachary G. Cuny

A Thesis Presented in partial fulfillment of

The Requirements for Graduation *Cursus Honorum*

Bachelor of Science Degree

Mississippi State University

April 2017

ACKNOWLEDGEMENTS

LIST OF TABLES

LIST OF FIGURES

NOMENCLATURE

ITC	Isothermal Titration Calorimetry
DSC	Differential Scanning Calorimetry
CD	Circular Dichroism
UV-Vis	Ultraviolet-Visible
PDS	Pyridostatin
K^+	Potassium Ion
KCl	Potassium Chloride Salt
BPES	Biphosphate EDTA Saline
KH_2PO_4	Monobasic Potassium Phosphate
K_2HPO_2	Dibasic Potassium Phosphate
EDTA	Ethylenediaminetetraacetic Acid
H_2O	Water
DI	Deionized; dissolved substances and ionized particles have been removed
PQS	Putative G-Quadruplex forming Sequence
^oC	Degrees Celsius (Temperature)
mM	Millimolar, 10^{-3} moles of solute per liter
μM	Micromolar, 10^{-6} moles of solute per liter
ΔG	Change in Gibbs Free Energy (in kcal/mol)

ΔH	Change in Enthalpy (in kcal/mol)
ΔS	Change in Entropy (in kcal/(mol*K))
K_a	Association Constant
K_d	Dissociation Constant

CHAPTER 1

INTRODUCTION

G-Quadruplexes as a Potential Anti-Cancer Target

When one thinks of DNA, the traditional image of the Watson and Crick double-helical structure typically comes to mind. However, this is not the only type of secondary structure that nucleic acids can adopt. Nucleic acids that are rich in runs of the nucleotide base guanine can form a non-canonical secondary structure known as a G-quadruplex. These structures are composed of two or more G-tetrads, square-planar motifs formed via a self-associating Hoogsteen hydrogen bonding network of four guanine DNA bases. These tetrads are stacked on top of each other and stabilized by π-π interactions between the guanine bases. G-quadruplex forming sequences can be found in both RNA and DNA, and quadruplexes can be composed of one or multiple nucleic acid strands. When formed from a single strand of nucleic acid (termed a unimolecular quadruplex), the structure acts as a knot. Non-quadruplex forming bases between runs of guanine will form loops on the ends or sides of the stacked tetrad core.

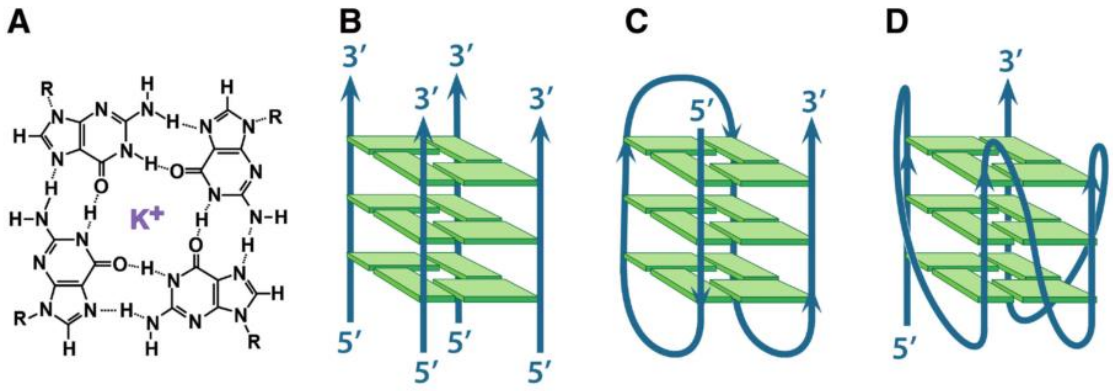

Figure 1.1: A) A G-tetrad depicting the Hoogsteen Hydrogen bonding network and stabilizing metal cation. The cation sits below or above the plane of the tetrad between tetrad layers, i.e. two metal cations per 3 tetrads. B) Tetramolecular parallel G-quadruplex. C) A unimolecular antiparallel G-quadruplex. D) A unimolecular parallel G-quadruplex.[1]

In recent years, G-quadruplex structures have been identified in both DNA and RNA as important regulatory structures in the cell, and they appear to control a diverse set of functions.[2] Putative G-quadruplex forming regions often appear in the promoter regions of known oncogenes including c-MYC,[3] BCL-2, [4] KRAS, [5] and c-kit,[6] providing an attractive target for anti-cancer therapies. DNA polymerase, the protein responsible for unraveling DNA during the replication process, does not have the ability to resolve (unwind) these structures during DNA replication; this will result in pausing at the G-quadruplex site. If stabilized exclusively in malignant cells, it is hypothesized that G-quadruplexes could cause DNA replication to prove fatal to the cell by inducing cell death through activation of DNA damage responses, or initiating cell-cycle arrest and inhibiting cell repair mechanisms.[7, 8, 9]

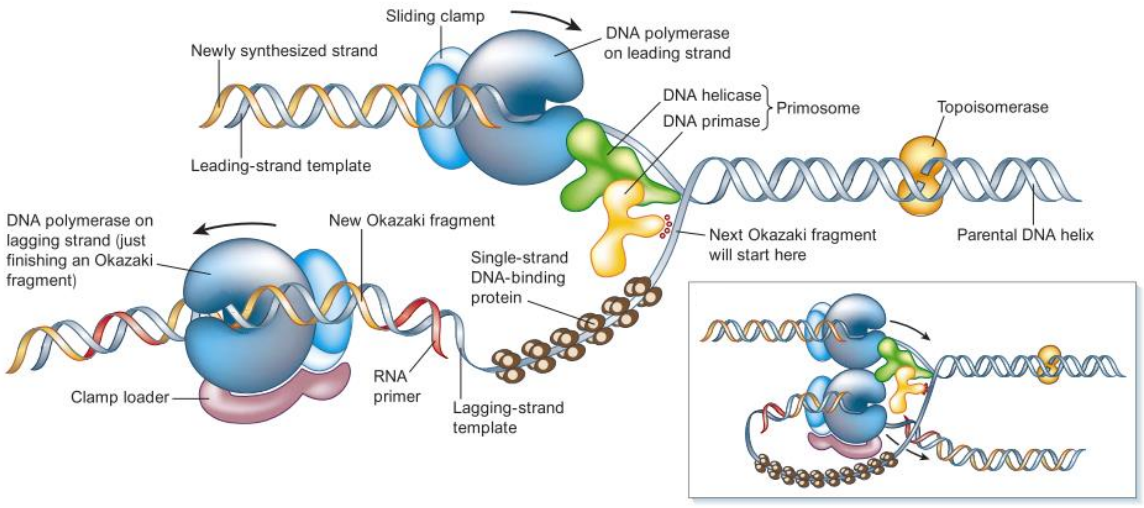

Figure 1.2: Diagram of the DNA replication complex unwinding and copying duplex DNA.[10]

Pyridostatin as a G-Quadruplex Binder

Pyridostatin (PDS) is a known G-quadruplex-specific binder designed to form a complex with telomeric G-quadruplexes and is believed to interfere with shelterin, which is a protein complex that protects the telomeric overhang of the nucleic DNA strand.[11-14] Without that protection of shelterin, the cell mistakes the telomeric overhang for a double-stranded DNA break, and histone H2AX is phosphorylated to DNA-damage response marker γ-H2AX.[15-17] When PDS abnormally activates the damage response mechanism, the cell will then trigger cell cycle arrest, DNA repair mechanisms, senescence, and apoptosis.[7-9, 12, 15-17] It is believed that PDS can cause the POT1 (Protection of Telomeres 1) region of the shelterin complex, the protein domain in

intimate contact with the single stranded overhang,[18-20] to become uncapped from the telomeric DNA resulting in a damage response.[11]

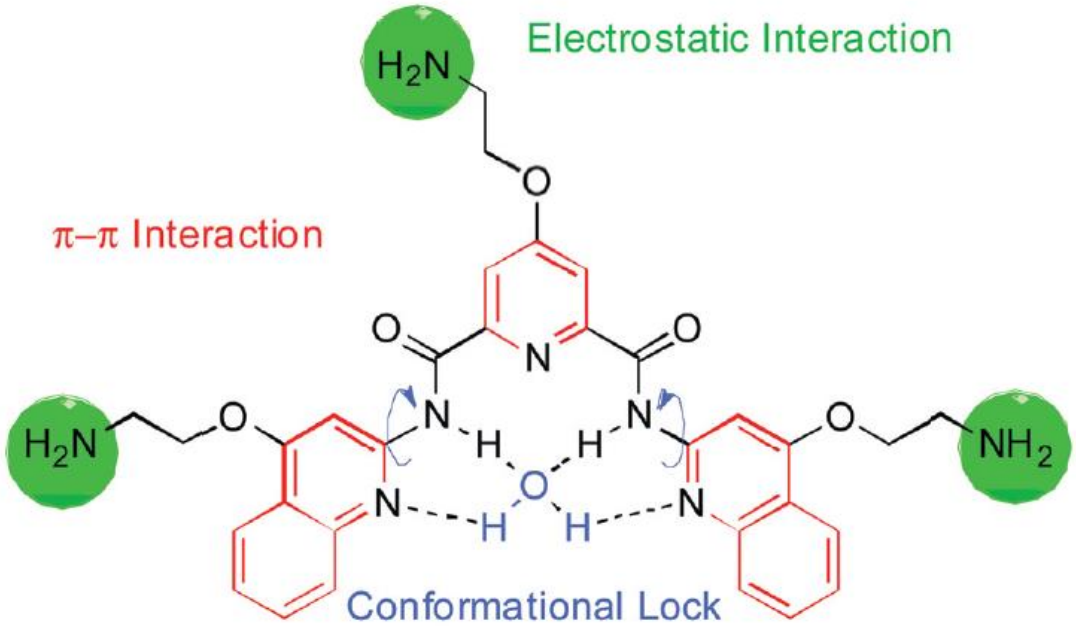

Figure 1.3: Molecular Structure of Pyridostatin. The design rationale is indicated on the structure.[21]

In 2012, it was demonstrated that the ligand had at least a 1:1 binding mode with quadruplex motifs[12] using NMR spectroscopy. Recently, it has also been shown that PDS can interact with irregular quadruplex structures[22], such as those that would have a loop length of 6 or more bases, or have a shunted-out base interrupting the tetrad stacking structure. This finding was a result of an experiment performed to identify and map out putative quadruplex-forming sequences (PQS) within DNA extracted from human B

lymphocytes. Over 700,000 PQS were identified, 400,000 of which were not predicted by computational methods. Those that were not predicted to form were mostly of these irregular types.

Previously, it was reported that PDS binds G4-DNA with an affinity (K_d) of 490 ± 80 nM.[24] This value is known as a dissociation constant, and is a measure of how likely a ligand is to be removed from a receptor. In contrast, an association constant (K_a), the inverse of this value, can be reported, and is a value of a ligand's affinity for a receptor. The smaller the value of K_d is, and similarly, how large the K_a is, the stronger the interaction between ligand and target. The above published value was obtained using a single molecule optical tweezers method, in which the mechanical stability of a quadruplex was evaluated in the presence and absence of PDS and calculating a dissociation constant for the interaction from the force required to pull apart the quadruplex by the 5' and 3' ends. This method appears to be effective at determining the binding affinity of a ligand-quadruplex complex in a single molecule setting, but it is only able to determine the mechanical stability of the quadruplex.

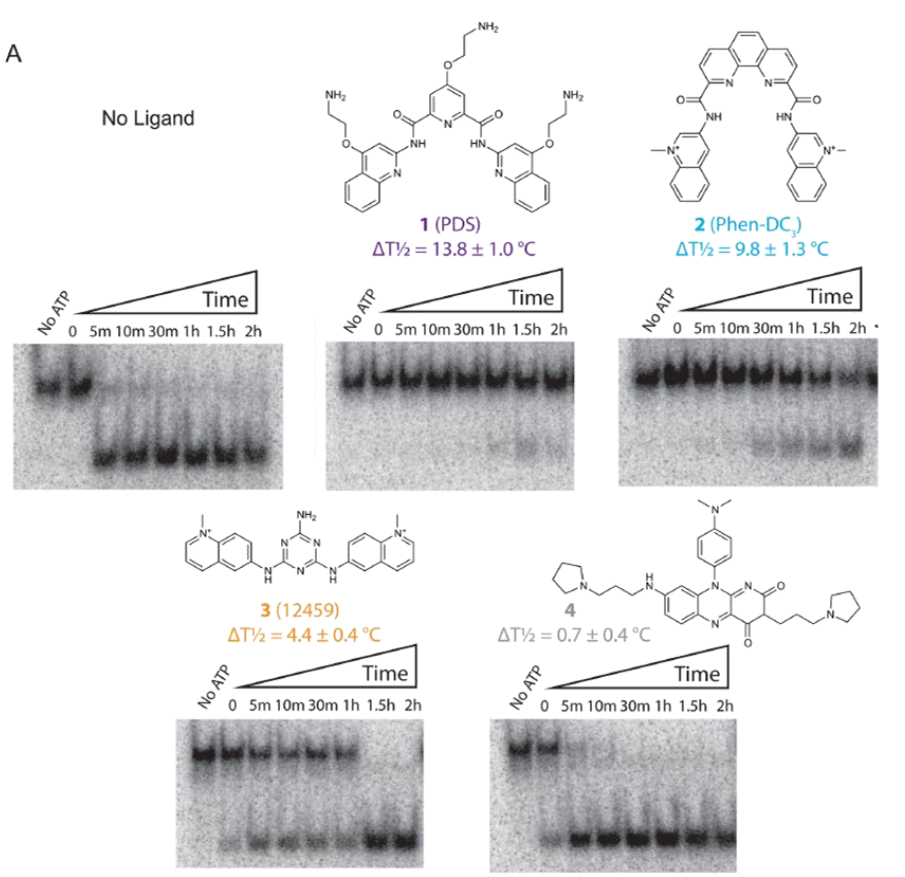

Figure 1.4: Molecular structures of previously reported G4-stabilizing ligands used in this study. G4 used was Z33, with the sequence: 5'-AAAGTGATGGTGGTGGGGGGAAGGATTTTCGAAC-3'. Differential transition temperature of the Z33 G4 with and without the presence of ligand is indicated below each respective structure. Polyacrylamide gels show the quantity of unwound G4 (lower band) as a result of the addition of the corresponding G4-stabilizing ligand at 5 M (above each gel).[22]

One of the most interesting effects of PDS is that it can allow G-quadruplexes to resist being unfolded (resolved) by the DHX36 gene product, G4R1 (G-quadruplex Resolvase 1).[22] This protein was discovered in 1997 and is the first structure known to resolve G-quadruplexes *in vivo*.[25, 26] Upon binding to the phosphate backbone of a

quadruplex structure, it will remain bound to the quadruplex until it reacts with ATP, at which point it will partially unwind the quadruplex, resulting in the structure either completely unfolding or reforming in solution. It was found that PDS could prevent this resolving activity in vitro more so than Phen-DC3, a ligand that binds to quadruplexes slightly weaker than PDS. PDS or a related analog may have promise as a potential cancer therapy via its interactions with G-quadruplexes.

Here, we will examine the thermodynamics for binding PDS to G-quadruplex structures from the c-MYC Nuclease Hypersensitivity Element ($NHE\text{-}III_1$) promotor region.

CHAPTER 2

MATERIALS AND METHODS

In this study, a variety of techniques were used, including Circular Dichroism (CD), Ultraviolet-Visible Spectroscopy (UV-Vis), and Isothermal Titration Calorimetry (ITC). This section contains a description of the oligonucleotide sequences that will model the c-MYC G-quadruplex, a brief description of the theory behind each technique, as well as a description of the experimental procedures.

Oligonucleotide Sequences

In this experiment, an oligonucleotide sequence for the c-MYC NHE-III_1 promotor region was examined and mutated to observe restricted folding topologies. The c-MYC gene is responsible for both cell proliferation, and apoptosis and forms a G-quadruplex due to its guanine-rich sequence.[28] The c-MYC NHE-III_1 promotor region is also responsible for about 80% of the gene's expression.[29] The wild-type (WT) sequence indicates that it has the potential to form multiple quadruplex structures; the major topologies will be a mixture characteristic of mutant quadruplexes 1-6-1 and 1-2-1 in solution, while favoring the formation of the 1-2-1 conformation.[30] The 1-2-1 conformation is also the most thermodynamically stable structure the WT sequence can form, so WT experimental results are likely to be very similar to results from experiments with the 1-2-1 sequence. The sequences are listed on the next page, with guanines potentially involved in tetrad formation underlined and in bold.

c-MYC Wild-Type (24-mer)

5’-TG**GGG**A**GGG**T**GGG**GA**GGG**T**GGG**GA-3’

c-MYC 1-2-1 Mutant (24-mer)

5’-TTTTTA**GGG**T**GGG**GA**GGG**T**GGG**GA-3’

c-MYC 1-6-1 Mutant (24-mer)

5’-TG**GGG**A**GGG**TTTTTA**GGG**T**GGG**GA-3’

Oligonucleotides were purchased from Midland Certified Reagent Company, Inc. (Midland, TX), and PDS was purchased as a trifluoroacetate salt from SelleckChem. Oligos were initially dialyzed in 1 L of 130 mM K^+ BPES buffer at pH 7.4 (100 mM KCl, 10 mM KH_2PO_4, 10 mM K_2HPO_4, and 1 mM EDTA) for approximately 36 hours. Buffer was replaced every 12 hours to remove any impurities from the DNA sample. After dialysis, the oligos were annealed by heating to 98 °C and then cooling by 2 °C every 15 minutes to 4 °C to allow the DNA to fold into its most stable quadruplex topology. The folded quadruplex solutions were exhaustively dialyzed in DI H_2O to remove salt not coordinated between with the G-tetrad faces. This resulted in parallel G-quadruplexes with K^+ ions stacked between tetrads dissolved in water, as shown in experimental data. These solutions were used as stock solutions for experiments. Dry PDS was dissolved in the DI H_2O dialysate to create stock solutions, and aliquots were diluted as necessary for experiments.

Initial experiments were performed in K^+ BPES buffer, but due to poor solubility of PDS, further experiments were performed in water. When buffer was added to solvate dry PDS, the solution turned a translucent blue-white color, and excess PDS crashed out of solution. A concentration above 50 μM could not be achieved, even in a 30% DMSO buffer solution. However, this was not the case when DI H_2O was used as the solvent. The solution remained clear, and concentrations in excess of 10 mM were achieved.

Introduction of Techniques

Isothermal Titration Calorimetry

Isothermal Titration Calorimetry (ITC) is commonly used to study the thermodynamic properties associated with the interaction of biological molecules, including protein-DNA/RNA interactions and small molecule-DNA interactions. Biochemical reactions involve either the evolution or absorption of heat, occurring due to the intermolecular interactions between the two compounds. A typical ITC instrument contains two cells, one of which contains a reference liquid (typically buffer or solvent) and the other containing the sample solution. A syringe placed in the sample cell injects small volumes of titrant solution into the sample. The cells are heated slightly above the enclosure temperature and the power input to the cells required to maintain a constant user defined temperature against the constant temperature sink is measured. Depending on the reaction being endergonic or exergonic, additional power will be applied to the sample cell or turned off. The power compensation (reported in μcalories) may be

integrated for each peak to determine the heat of injection per mol of ligand. Nonlinear regression fitting of the resulting titration curve provide a direct measure of enthalpy at each point and may be used to determine the K_a which may be expressed as Gibbs Free Energy through the equation:

$$\Delta G = -RTln(K)$$

Knowing K_a from the non-linear regression fit and ΔH from the injection heats the entropy of the reaction may be determined by the following equation.

$$\Delta G = \Delta \mathrm{H} - T\Delta S$$

Circular Dichroism

Circular Dichroism (CD) is a technique in which left and right circularly polarized light is passed through a sample to measure the differential absorption of light. The structural asymmetry of a molecule will determine which polarization it will absorb, allowing the structure of macromolecules to be determined. If a molecule is not asymmetrical, it will not produce a CD signal. This technique was utilized to identify structural changes in G-quadruplex DNA resulting from PDS binding.

Ultraviolet-Visible Spectroscopy

Some molecules will absorb light in the ultraviolet range of the electromagnetic spectrum, including biological molecules. UV-vis is commonly used to verify the concentration of DNA and the ligand samples (if the ligand is UV active). This technique involves illuminating a sample with light over a specific range of wavelengths, and then monitoring which wavelengths of light are not passed through the sample. Data is then

plotted in the form of absorbance vs. wavelength. DNA will have a maximum absorbance at 260 nm, and PDS will have its strongest peak present at 227 nm. Application of the Beer-Lambert equation allows for the determination of the concentration of samples.

Experimental Procedures

ITC Experiments

Experiments were performed using a VP-ITC Calorimeter (GE-Healthcare). A typical experiment consisted of 35 8 μL injections performed at 25ºC. The cell contained 1.4 mL of 15 μM DNA, and a syringe held 280 μL of 1 mM PDS. These parameters were applied to all titrations for all sequences. Due to the nature of the synthesis of PDS, the stock solution was a slight acetate solution, meaning that a buffer mismatch will occur during our titration. The heat of dilution was accounted for by performing a "blank" titration, in which only PDS was titrated into 18 MΩ-cm water. The integrated heat values for this titration were subtracted from the experimental values so that only the heat from the PDS/quadruplex interaction is present. ITC thermograms were plotted using Origin, the baseline corrected and blank titration (1 mM PDS titrated into dialysate) subtracted from the ligand-DNA titrations. Data were analyzed using CHASM, a nonlinear regression algorithm program developed previously in our laboratory.[31] Experiments were performed in triplicate and errors reported as one standard deviation from the mean.

CD Experiments

CD experiments were performed using an OLIS DSM 20 Spectrophotometer (Bogart, GA). Temperature was controlled at 25°C using a Quantum Northwest TC125 Temperature Control unit. A baseline scan was performed over a spectral range of 220-420 nm on a sample of 2000 μL DI H_2O dialysate in a 1 cm quartz cuvette. The cuvette was transferred to a Hewlett-Packard 8452A Diode Array UV-Vis spectrophotometer, and a scan was taken over the same range and used as a reference scan. DNA was added until an absorbance of ~0.9-1.0 AU at 260 nm was observed. The cuvette was then transferred back to the CD spectrophotometer, and a scan was taken after temperature equilibration. Titrations were performed by adding small aliquots of a 2.5 mM PDS solution (concentration verified by UV-Vis) into the DNA sample, mixing well, and incubating for 5 minutes to ensure the sample was temperature equilibrated and binding reactions are complete. Blank scans were performed by repeating the experiment in the absence of DNA and subtracting the data from the corresponding DNA titration. Results were analyzed using the Olis Globalworks program. Corrected spectra were converted to Molar Ellipticity using Microsoft Excel, and then baseline zeroed at 320 nm or 290 nm. The data was plotted using Graphpad Prism. Subtraction of a linear best fit line to correct baseline drift was applied when necessary. Each experiment was performed in duplicate.

CHAPTER 3

RESULTS AND DISCUSSION

CD Studies

Initial scans of all sequences showed signals in the spectra that were characteristic of the presence of Type I conformation G-quadruplexes in solution.[32] The characteristic peaks are a negative signal at 240 nm and a positive signal at 260 nm which confirms that G-quadruplex structure is present in the DI H_2O. Upon the addition of a 1:1 mole ratio of PDS into c-MYC WT DNA, CD signal attenuated slightly. Further attenuation was observed at the 2:1 mol ratio PDS:DNA where the signal remained relatively constant upon additional PDS. This resistance in attenuation in excess of 2:1 binding is suggestive of 2 molecules of PDS binding per molecule of G-quadruplex, with excess pds binding nonspecifically or not at all.

c-MYC 1-2-1 demonstrated attenuation to a much larger extent than the WT complex upon PDS titrations, potentially resulting from the less dynamic accessible topologies and short loops. Upon addition of 1:1 mole ratio PDS, the molar ellipticity demonstrated an attenuation. Attenuation to a similar magnitude was observed for the addition of the second equivalence of PDS. Continuous attenuation as a result of ligand binding was seen over the entire course of this titration. Clearly either PDS is acting to disrupt the structure of the c-MYC 1-2-1 G-quadruplex, though to a greater extent than is seen in c-MYC WT.

Interestingly, the CD spectra for the 1-6-1 mutant does not follow this trend. The careful observer may note that the c-MYC 1-6-1 peak at 260 nm is not as symmetrical as the WT or 1-2-1 mutants. Upon reaching a 2:1 PDS:DNA ratio, a peak at about 290 nm becomes more prominent, while the peak at 260 nm attenuates. A likely interpretation of this data is that the 1-6-1 mutant contains a small population of G-quadruplexes with antiparallel character and the PDS shifts the equilibrium to favor the antiparallel conformation. These spectra at higher PDS:DNA ratios are indicative of the adoption of Type II quadruplex structure.[32] Type II antiparallel G-quadruplexes contain a tetrad containing bases of a different glycosidic bond angle (GBA) than the other two tetrads. It is possible that due to the larger loop length of this mutant, the interaction of this quadruplex with PDS encourages the quadruplex population to refold into a structure with more antiparallel character, and during the process, allow for some bases to reorient their GBA from Head-to-Tail stacking to either Head-to-Head or Tail-to-Tail stacking. Attenuation of this spectra at 260 nm is likely due to this reorganization of structure as well. This result was not observed in either the wild-type or 1-2-1 spectra.

Previous literature has also reported a topology shift in G-quadruplexes from Type II antiparallel to Type III antiparallel, in which all tetrads have Head-to-Head and Tail-to-Tail stacking.[14] Marchand et. al. reported CD spectra in which a 1:1 PDS:DNA mole ratio was achieved, and after incubation, the unimolecular quadruplex adopted the spectra characteristic of a Type III quadruplex, as characterized by a shift from a negative to a positive signal and from a positive to a negative signal at 240 and 260 nm

respectively, while retaining a strong positive signal at 290 nm. This indicates that the guanines making up the quadruplex had alternating GBAs such that stacking was Head-to-Head or Tail-to-Tail in all cases. Our spectra of the 1-6-1 shows a similar phenomenon through the increased magnitude of the 290 nm peak in our experimental spectra. However, this did not become obvious until a 2:1 mole ratio was achieved, rather than the 1:1 ratio described by Marchand.[14]

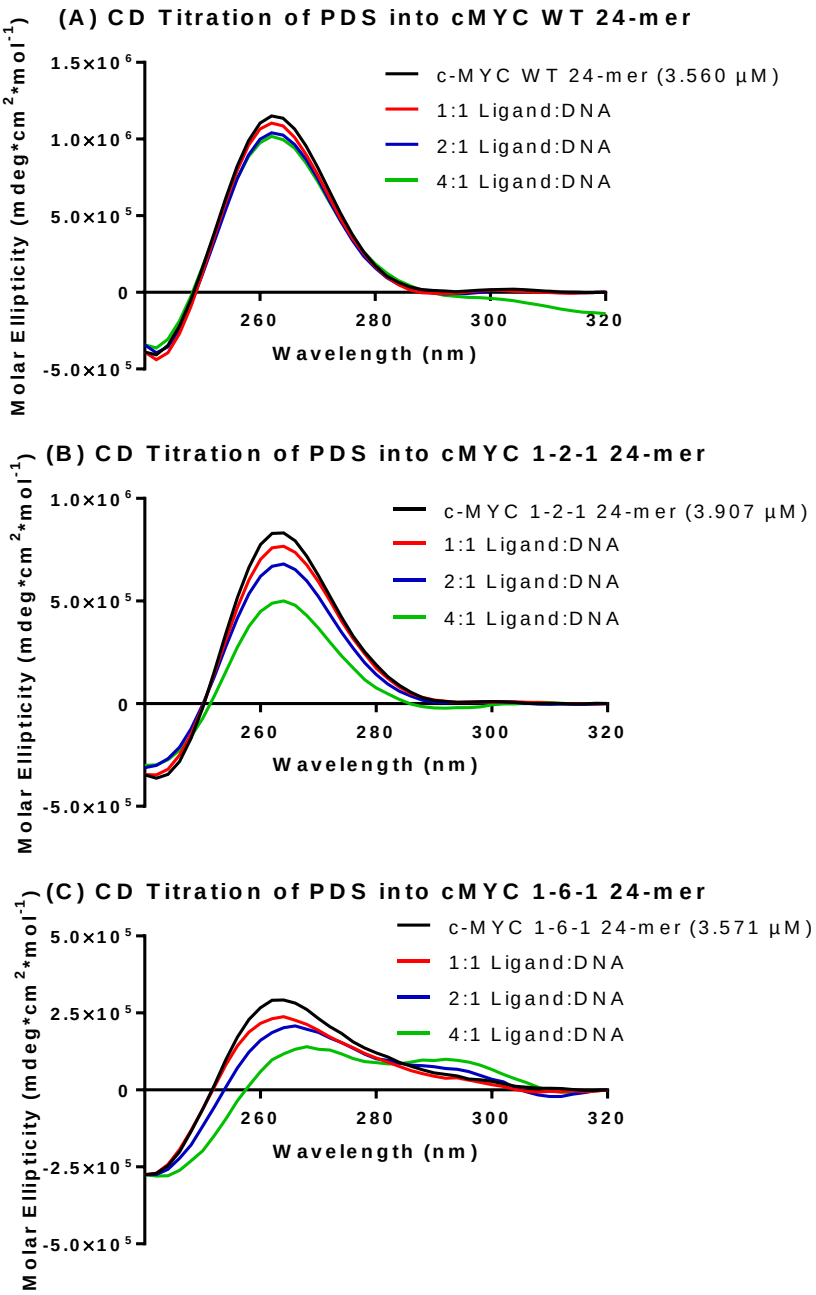

Figure 3.1.1 CD Spectra of PDS titrated into G4 DNA solutions. (A) c-MYC WT 24-mer; (B) c-MYC 1-2-1 24-mer; and (C) c-MYC 1-6-1 24-mer

ITC Studies

Titrations were fit to a single binding mode model, in which a single PDS molecule will bind to either exposed tetrad face of the quadruplex in a primarily enthalpy driven binding event. This model is supported by a calculated n value of about 2 and negative ΔG values as a result of large, negative ΔH values indicating an exothermic process, and smaller unfavorable $-T\Delta S$ values.

PDS titrations of the c-MYC 1-2-1 quadruplex exhibited the largest K_a values, corresponding to the tightest binding. This binding mode had the same enthalpy contribution as the 1-6-1 G-quadruplex but was a tighter binder due to the reduced entropic penalty. This reduced penalty likely is due to loop interactions with PDS. The c-MYC 1-6-1 G-quadruplex pays a larger entropic penalty to bind PDS and exhibits the weakest affinity of the G-quadruplex samples examined in this work.

The WT G-quadruplex exhibits an average affinity of -9.6 $kcal*mol^{-1}$ which is approximately equivalent, within error, to the mutants from which it is comprised. PDS clearly binds with similar tight affinity and a very similar thermodynamic profile to all of the examined c-MYC quadruplexes. Calorimetric determination of binding thermodynamics is a direct method of determining K_a, whereas the molecular tweezers approach indirectly determines K_a via changes in complex stability. PDS binding to each quadruplex in this work demonstrated tighter binding than the of 208 x 10^4 M determined using the indirect molecular tweezer approach and a human telomeric quadruplex.[24] The

calorimetric K_a was tighter typically by about an order of magnitude than that determined by the molecular tweezer approach.

Mutant Type	Mode	n	K_a x 10^{-4}	ΔG (kcal/mol)	ΔH (kcal/mol)	-TΔS (kcal/mol)
WT	1	2.1 ± 0.1	1030 ± 120	-9.6 ± 0.1	-12.0 ± 0.8	2.4 ± 0.9
1-2-1	1	2.1 ± 0.1	1900 ± 800	-9.9 ± 0.3	-12.70 ± 0.03	2.8 ± 0.2
1-6-1	1	2.04 ± 0.03	400 ± 50	-9.3 ± 0.1	-12.7 ± 0.5	3.5 ± 0.4

Table 3.2.1) Thermodynamic Profiles of observed binding events for PDS binding to G4 DNA.

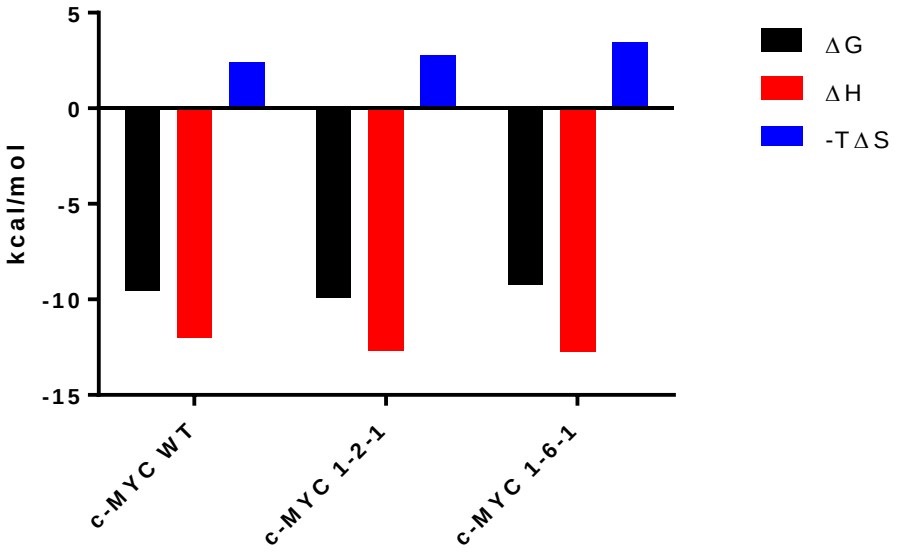

Figure 3.2.1) Visual Representation of Thermodynamic Profiles. ΔG values are black bars, ΔH values are red bars, and –TΔS values are blue bars.

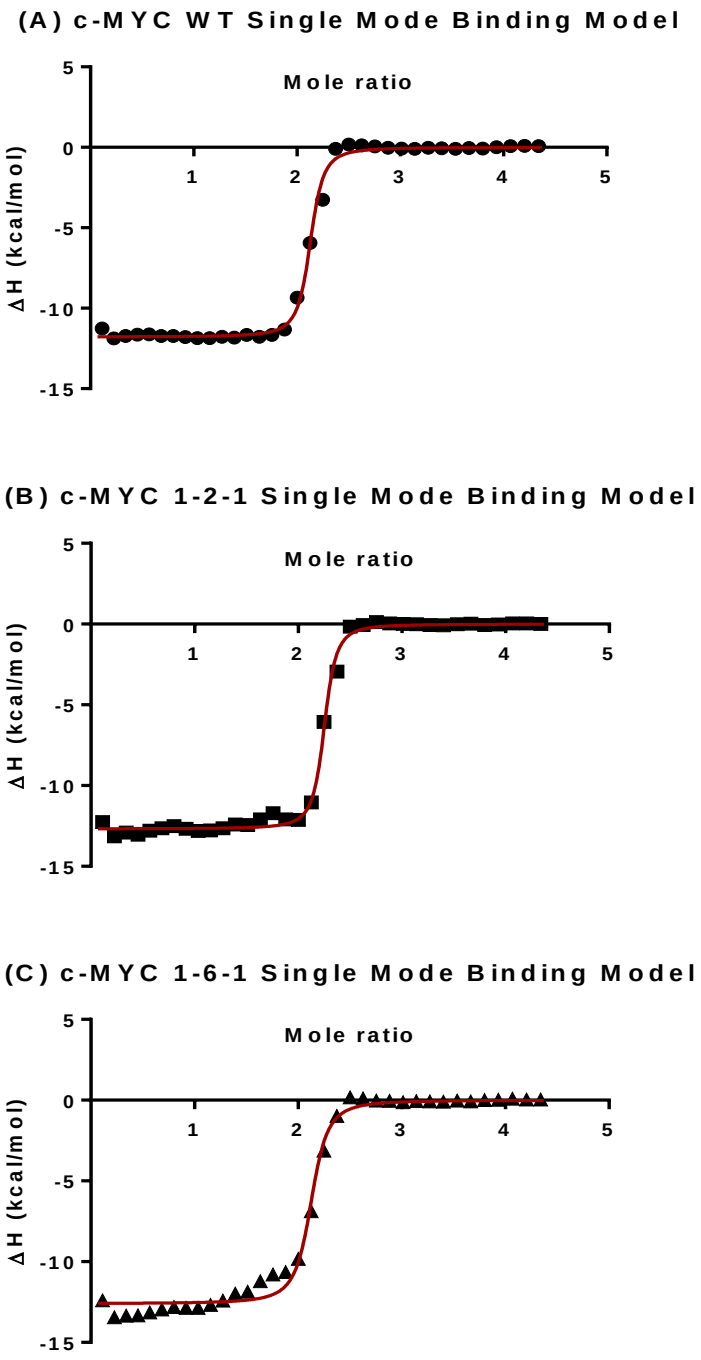

Figure 3.2.2) ITC Thermograms with mathematical fits overlaid on the data. (A) Wild Type; (B) 1-2-1; (C) 1-6-1.

CHAPTER 4

SUMMARY AND CONCLUSION

In conclusion, we were able to observe PDS' interactions with c-MYC G-quadruplexes. As observed in the CD spectra, upon addition of PDS, there is an attenuation of molar ellipticity at 260 nm in all spectra. This is most apparent in the case of the 1-2-1 mutant. This loss of signal is indicative of a loss of G-quadruplex structure in solution, and can be attributed to complexation with PDS. A peak at 290 nm becomes more apparent in the 1-6-1 spectra, indicative of a conformational change from a Type I parallel quadruplex with consistent Head-to-Tail guanine orientations throughout the quadruplex, to a Type II antiparallel quadruplex characterized by one tetrad having guanines that reorient to either a Head-to-Head or a Tail-to-Tail stacking conformation while the other two tetrads retain their original conformations.

ITC thermograms were fit to a single binding mode model, in which a single PDS binds to either exposed tetrad face of the quadruplex. This model is supported by favorable ΔG values, an n value of 2, and a favorable enthalpic contribution. PDS binding demonstrated tighter binding than reported previously.

REFERENCES

1. Giri, B.; Smaldino, P. J.; Thys, R. G.; Creacy, S. D.; Routh, E. D.; Hantgan, R. R.; Lattmann, S.; Nagamine, Y.; Akman, S. A.; Vaughn, J. P., G4 resolvase 1 tightly binds and unwinds unimolecular G4-DNA. *Nucleic Acids Res* **2011,** *39* (16), 7161-78.
2. Lattmann, S.; Stadler, M. B.; Vaughn, J. P.; Akman, S. A.; Nagamine, Y., The DEAH-box RNA helicase RHAU binds an intramolecular RNA G-quadruplex in TERC and associates with telomerase holoenzyme. *Nucleic Acids Res* **2011,** *39* (21), 9390-404.
3. Gonzalez, V.; Hurley, L. H., The c-MYC NHE III(1): function and regulation. *Annual review of pharmacology and toxicology* **2010,** *50*, 111-29.
4. Dai, J.; Dexheimer, T. S.; Chen, D.; Carver, M.; Ambrus, A.; Jones, R. A.; Yang, D., An intramolecular G-quadruplex structure with mixed parallel/antiparallel G-strands formed in the human BCL-2 promoter region in solution. *J Am Chem Soc* **2006,** *128* (4), 1096-8.
5. Cogoi, S.; Xodo, L. E., G-quadruplex formation within the promoter of the KRAS proto-oncogene and its effect on transcription. *Nucleic Acids Res* **2006,** *34* (9), 2536-49.
6. Gao, X.; Ma, W.; Nie, J.; Zhang, C.; Zhang, J.; Yao, G.; Han, J.; Xu, J.; Hu, B.; Du, Y.; Shi, Q.; Yang, Z.; Huang, X.; Zhang, Y., A G-quadruplex DNA structure resolvase, RHAU, is essential for spermatogonia differentiation. *Cell Death Dis* **2015,** *6*, e1610.
7. McLuckie, K. I.; Di Antonio, M.; Zecchini, H.; Xian, J.; Caldas, C.; Krippendorff, B. F.; Tannahill, D.; Lowe, C.; Balasubramanian, S., G-quadruplex DNA as a molecular target for induced synthetic lethality in cancer cells. *J Am Chem Soc* **2013,** *135* (26), 9640-3.
8. Ohnmacht, S. A.; Neidle, S., Small-molecule quadruplex-targeted drug discovery. *Bioorg Med Chem Lett* **2014,** *24* (12), 2602-12.
9. Bidzinska, J.; Cimino-Reale, G.; Zaffaroni, N.; Folini, M., G-quadruplex structures in the human genome as novel therapeutic targets. *Molecules* **2013,** *18* (10), 12368-95.
10. Alberts, B., DNA replication and recombination. *Nature* **2003,** *421* (6921), 431-435.
11. Rodriguez, R.; Muller, S.; Yeoman, J. A.; Trentesaux, C.; Riou, J. F.; Balasubramanian, S., A novel small molecule that alters shelterin integrity and

triggers a DNA-damage response at telomeres. *J Am Chem Soc* **2008,** *130* (47), 15758-9.
12. Rodriguez, R.; Miller, K. M.; Forment, J. V.; Bradshaw, C. R.; Nikan, M.; Britton, S.; Oelschlaegel, T.; Xhemalce, B.; Balasubramanian, S.; Jackson, S. P., Small-molecule-induced DNA damage identifies alternative DNA structures in human genes. *Nat Chem Biol* **2012,** *8* (3), 301-10.
13. Murat, P.; Gormally, M. V.; Sanders, D.; Di Antonio, M.; Balasubramanian, S., Light-mediated in cell downregulation of G-quadruplex-containing genes using a photo-caged ligand. *Chem Commun (Camb)* **2013,** *49* (76), 8453-5.
14. Marchand, A.; Granzhan, A.; Iida, K.; Tsushima, Y.; Ma, Y.; Nagasawa, K.; Teulade-Fichou, M. P.; Gabelica, V., Ligand-induced conformational changes with cation ejection upon binding to human telomeric DNA G-quadruplexes. *J Am Chem Soc* **2015,** *137* (2), 750-6.
15. Podhorecka, M.; Skladanowski, A.; Bozko, P., H2AX Phosphorylation: Its Role in DNA Damage Response and Cancer Therapy. *J Nucleic Acids* **2010,** *2010*.
16. Dickey, J. S.; Zemp, F. J.; Altamirano, A.; Sedelnikova, O. A.; Bonner, W. M.; Kovalchuk, O., H2AX phosphorylation in response to DNA double-strand break formation during bystander signalling: effect of microRNA knockdown. *Radiat Prot Dosimetry* **2011,** *143* (2-4), 264-9.
17. Rogakou, E. P.; Pilch, D. R.; Orr, A. H.; Ivanova, V. S.; Bonner, W. M., DNA double-stranded breaks induce histone H2AX phosphorylation on serine 139. *J Biol Chem* **1998,** *273* (10), 5858-68.
18. Choi, K. H.; Farrell, A. S.; Lakamp, A. S.; Ouellette, M. M., Characterization of the DNA binding specificity of Shelterin complexes. *Nucleic Acids Res* **2011,** *39* (21), 9206-23.
19. Xin, H.; Liu, D.; Songyang, Z., The telosome/shelterin complex and its functions. *Genome Biol* **2008,** *9* (9), 232.
20. de Lange, T., Shelterin: the protein complex that shapes and safeguards human telomeres. *Genes Dev* **2005,** *19* (18), 2100-10.
21. Muller, S.; Sanders, D. A.; Di Antonio, M.; Matsis, S.; Riou, J. F.; Rodriguez, R.; Balasubramanian, S., Pyridostatin analogues promote telomere dysfunction and long-term growth inhibition in human cancer cells. *Org Biomol Chem* **2012,** *10* (32), 6537-46.
22. Chen, M. C.; Murat, P.; Abecassis, K.; Ferre-D'Amare, A. R.; Balasubramanian, S., Insights into the mechanism of a G-quadruplex-unwinding DEAH-box helicase. *Nucleic Acids Res* **2015,** *43* (4), 2223-31.

23. Chambers, V. S.; Marsico, G.; Boutell, J. M.; Di Antonio, M.; Smith, G. P.; Balasubramanian, S., High-throughput sequencing of DNA G-quadruplex structures in the human genome. *Nat Biotechnol* **2015,** *33* (8), 877-81.
24. Koirala, D.; Dhakal, S.; Ashbridge, B.; Sannohe, Y.; Rodriguez, R.; Sugiyama, H.; Balasubramanian, S.; Mao, H., A single-molecule platform for investigation of interactions between G-quadruplexes and small-molecule ligands. *Nat Chem* **2011,** *3* (10), 782-7.
25. Harrington, C.; Lan, Y.; Akman, S. A., The identification and characterization of a G4-DNA resolvase activity. *J Biol Chem* **1997,** *272* (39), 24631-6.
26. Vaughn, J. P.; Creacy, S. D.; Routh, E. D.; Joyner-Butt, C.; Jenkins, G. S.; Pauli, S.; Nagamine, Y.; Akman, S. A., The DEXH protein product of the DHX36 gene is the major source of tetramolecular quadruplex G4-DNA resolving activity in HeLa cell lysates. *J Biol Chem* **2005,** *280* (46), 38117-20.
27. Kwok, C. K.; Balasubramanian, S., Targeted Detection of G-Quadruplexes in Cellular RNAs. *Angew Chem Int Ed Engl* **2015,** *54* (23), 6751-4.
28. Chen, S.; Su, L.; Qiu, J.; Xiao, N.; Lin, J.; Tan, J. H.; Ou, T. M.; Gu, L. Q.; Huang, Z. S.; Li, D., Mechanistic studies for the role of cellular nucleic-acid-binding protein (CNBP) in regulation of c-myc transcription. *Biochim Biophys Acta* **2013,** *1830* (10), 4769-77.
29. Dang, C. V., c-Myc target genes involved in cell growth, apoptosis, and metabolism. *Mol Cell Biol* **1999,** *19* (1), 1-11.
30. Dettler, J. M.; Buscaglia, R.; Le, V. H.; Lewis, E. A., DSC Deconvolution of the Structural Complexity of c-MYC G-Quadruplexes. *Biophys. J.* **2011**, 100(6), 1517-1525.
31. Le, V. H.; Buscaglia, R.; Chaires, J. B.; Lewis, E. A., Modeling complex equilibria in isothermal titration calorimetry experiments: thermodynamic parameters estimation for a three-binding-site model. *Anal Biochem* **2013,** *434* (2), 233-41.
32. Randazzo, A.; Spada, G. P.; da Silva, M. W., Circular dichroism of quadruplex structures. *Top Curr Chem* **2013,** *330*, 67-86.